PAPER

Check for updates

Manufacturing process significantly impacts the rate of degradation of polylactic acid (PLA) under controlled composting conditions

Jennie O'Loughlin,[a] Hannah McDonnell,[a] Robyn Lawless,[a] Susan M. Kelleher, [b] Samantha Fahy,[c] Brian Freeland,[d] Keith D. Rochfort [*de] and Jennifer Gaughran[a]

Bioplastic usage is increasing steadily to combat the negative environmental impacts associated with traditional, petrochemical-based plastics. Global bioplastics production is set to increase from 2.18 million tonnes in 2023 to 7.43 million tonnes by 2028. Polylactic acid (PLA) is the leading bioplastic on the market, with 31% of the global market share in 2023. With an increase in the use of PLA forecast for the near future, it is imperative to understand the real-world end-of-life options for this polymer. In this work, the effect of 3D printing *versus* injection moulding on the disintegration rates of PLA labware components was investigated. Commercially available PLA granules were 3D-printed using fused deposition modelling or injection moulded. 3D-printed PLA specimens showed an increased rate of disintegration (>90% after 12 weeks) under industrial composting conditions compared to the injection moulded specimens (∼54% disintegration after 12 weeks). The effect of mechanical recycling of neat PLA on disintegration rate was also investigated. PLA that had undergone mechanical recycling three times showed a slight increase in the rate of disintegration. The impact of surface topography and manufacturing method on the rate of disintegration of PLA is comprehensively studied through various analytical techniques (GPC, DSC, FTIR, SEM, and profilometry). This study provides insights into the effect of processing and postprocessing techniques on the real-life applications and end-of-life options of PLA components. The importance of component design and production method when developing 'biodegradable' alternative plastics is highlighted.

Sustainability spotlight

Polylactic acid (PLA), a biodegradable bioplastic, has recently emerged as a suitable material for bioscience labware components. This study investigated the degradability of PLA-based labware, produced *via* 3D-printing (fused deposition modelling) and injection moulding. An in-depth chemical analysis revealed significant differences in disintegration rates between manufacturing methods. 3D-printed PLA disintegrated more rapidly under industrial composting conditions, due to its greater surface area and increased water sorption. This research also assessed practical end-of-life scenarios; mechanical recycling and autoclave sterilization prior to composting accelerated PLA disintegration, highlighting methods to improve the degradation of PLA materials post-use. By addressing real-world disposal and reuse strategies, this work supports UN SDG 12 and 13, emphasizing the importance of design and processing when developing sustainable products.

1. Introduction

In 2023, 413.8 million tonnes of plastic was produced globally,[1] with bioplastics making up an estimated 0.5%.[2,3] Global bioplastics production is estimated to increase from 2.18 million tonnes in 2023 to 7.43 million tonnes by 2028.[2] The increased interest in bioplastic production and usage is an effort to

combat the negative effects of traditional, petrochemical-based plastics, which are poorly degraded in the environment, resulting in wide ranging environmental pollution.[4–6] Bioplastics can be produced from renewable resources, such as food crops[7] and/or are biodegradable.[8] It has been shown that bioplastics can result in a 14–69% reduction in CO_2eq per kg (carbon emissions equivalent per kilogram), depending on the traditional fossil fuel-based plastic being replaced and the weight of plastic product.[9] Polylactic acid (PLA) is the leading bioplastic on the market, mainly for single-use and short shelf-life products,[10–12] due to its advantageous mechanical and physicochemical properties and the ease of processability during injection moulding and 3D printing.[13,14] With the move

[a]*School of Physical Sciences, Dublin City University, D9 Dublin, Ireland*
[b]*School of Chemical Sciences, Dublin City University, D9 Dublin, Ireland*
[c]*Office of the Chief Operations Officer, Dublin City University, D9 Dublin, Ireland*
[d]*School of Biotechnology, Dublin City University, D9 Dublin, Ireland. E-mail: keith. rochfort@dcu.ie; Tel: +353 700 7775*
[e]*Life Sciences Institute, Dublin City University, D9 Dublin, Ireland*

towards reducing plastic production and waste worldwide, from the United Nations Environment Programme's resolution to end plastic pollution,[15] to the Council of the European Union's 'Packaging and Packaging Waste Regulation 2024',[16] the end-of-life options of relatively novel bioplastics such as PLA must be considered.

The biodegradation of PLA films and extruded products have been studied under thermophilic composting conditions[17–20] and under aquatic conditions.[21,22] PLA undergoes biodegradation under aerobic conditions to produce biomass, CO_2, and H_2O, and under anaerobic conditions to produce biomass, CO_2, H_2O, and CH_4.[23] PLA degradation is predominated by hydrolytic chain scission of the ester bonds upon exposure to water molecules, resulting in oligomers.[24,25] The biodegradation rate of PLA can vary depending on molecular weight, optical purity (D/L ratio), degree of crystallinity, and temperature and humidity of the environment.[25] The literature provides extensive insights into PLA biodegradation in various environments (compost, soil, landfill, water) and it is indicated that compost results in the fastest rate of PLA biodegradation.[26] There have also been studies investigating both biotic and abiotic methods to improve PLA degradation under various environmental conditions.[27] Certain abiotic methods have been found to increase the rate of PLA degradation. These include during-processing techniques such as the addition of degradable additives[28,29] or before degradation processing such as chemical hydrolysis in alkaline solution[30] or gamma irradiation.[31] Recently, a PLA–pectin plasticizer composite was found to exhibit improved and controlled hydrolytic degradation in alkaline, acidic, and neutral solutions, although this study did not investigate the composite's degradation in compost.[32] The effects of PLA's internal structure on degradation have also been studied.[33] Amorphous PLA thin films (thickness = 195.5 μm) were mechanical treated prior to composting to produce a film with a thickness of 95 μm, a film with increased crystallinity (20%), and a film that had undergone orientational stretching. The PLA films showed similar disintegration rates, although the amorphous film of 95 μm thickness had completely degraded after 21 days. Biotic methods to improve PLA's overall biodegradability have also been well studied. PLA films showed increased rates of biodegradation over a 90 day trial in compost at 58 °C that had been bioaugmented with the bacterial strain *Geobacillus thermoleovorans*.[34] This was monitored by the evolution of CO_2 during the trial, as a final by-product of PLA biodegradation. This study seeks to investigate the impact of surface topography on the initial stage of PLA degradation, as the impacts of polymer M_W and crystallinity in particular have been thoroughly investigated in the literature.[35–38] With this in mind, the PLA materials under investigation in this study were produced using two distinct manufacturing techniques, fused deposition modelling (3D-printing) and injection moulding.

Current PLA waste streams direct the material to industrial composting facilities, where aerobic, thermophilic (55–60 °C) and high moisture (60% w/w) conditions predominate. These conditions will therefore be the focus of this research. Bioplastics must meet international standards, such as ISO 17088 and EN 14995, to be considered 'compostable'. Under these guidelines, compostable materials must meet three parameters: (1) at least 90% 'disintegration' after 12 weeks, (2) at least 90% 'biodegradation' after 24 weeks, and (3) no negative effects on compost quality.[39] 'Disintegration' is defined as fragmentation of the plastic product into pieces of less than 2×2 mm in size. In the case of PLA, disintegration is initiated by hydrolytic cleavage of the ester groups, resulting in lower molecular weight polymer chains.[40,41] 'Biodegradation' is the conversion of the shorter chain polymers or oligomers into CO_2 and H_2O by microorganisms. This process is thought to occur in three stages; biofilm formation, depolymerization, and mineralization.[8] Several factors are known to affect the rate of plastic degradation, including material surface topography, molecular weight, and percentage crystallinity, as well as the environmental conditions such as humidity, temperature, oxygen levels, and medium pH.[42–44] Industrial composting facilities are often hesitant to accept PLA products, as the degradability of the PLA material can vary depending on product type (*i.e.* drinking bottle, disposable cutlery) and on the industrial operations not aligning with laboratory testing.[45] Very recently, studies have highlighted the potentially misleading labelling of commercially available bioplastic products,[46,47] where the final composition and/or production method leads to an 'environmentally friendly' end product that does not meet international composting standards. This work will investigate the effect of processing and postprocessing methods on the disintegration of PLA under industrial composting conditions, as outlined in ISO 20200:2023, 'Determination of the degree of disintegration of plastic materials under composting conditions in a laboratory-scale test'.[48]

Mechanical processing of polymers is often preferred in large-scale applications, as a cost-effective and sustainable option.[49] The use of recycled polymers in 3D-printing for rapid prototyping and CAD modelling is developing as an approach to manage plastic waste.[50] Mechanical recycling of PLA has been shown to have the lowest environmental impact as an end-of-life option, when a life cycle assessment was carried out comparing mechanical recycling, chemical recycling, and composting as means of disposal of PLA.[51] The effects of mechanical recycling on the mechanical and thermal properties of PLA have also been studied.[52–55] PLA specimens were produced using fused deposition modelling (FDM), 3D printing in all such studies and a lower tensile strength for the recycled PLA specimens was reported compared to virgin PLA. One study investigated recycling PLA up to three times, using injection moulding as the manufacturing process for the end specimens. This study found a slight decrease (14%) in tensile strength and a slight increase in the rate of disintegration in compost after each recycling round.[13] 3D printing as a manufacturing technology is an attractive production method, with associated waste reduction and rapid prototyping.[56] However, high energy demand and limited recyclability of 3D-printed materials has been highlighted.[57,58] Printing parameters can be defined, such as layer thickness, layer height, and infill patterns which all effect the resulting 3D-printed product.[59]

It has been estimated that single-use plastics (SUPs) in life science laboratories account for approximately 5.5 million

tonnes of waste per year globally.[60] The use of PLA as a replacement material for single-use plastic labware in the life sciences laboratory has previously been reviewed,[61,62] in an effort to reduce the reliance on fossil fuel-based SUPs in bioscience research laboratories. 3D-printed PLA products have previously been designed and manufactured.[61,62] In this work, the end-of-life options for PLA products are investigated, focusing on the disintegration of selected PLA materials under controlled composting conditions in this initial study. PLA is mechanically recycled repetitively until loss of material integrity. The disintegration of 3D-printed recycled PLA specimens is investigated, as well as virgin PLA specimens produced using injection moulding and distinct 3D printing infill patterns. The PLA specimens are also autoclaved (steam, 121 °C, 15 psi, 15 min), as this is an essential step in the waste stream of bioscience labware, if incineration of the labware is not the final step. A method registered by a patent utilized steam autoclaving to accelerate the rate of PLA degradation, as determined by the increased reduction of PLA M_W.[27,63] The impact of the various PLA processing methods on composting rate are compared using percentage disintegration as well as analytical techniques such as gel permeation chromatography (GPC), differential scanning calorimetry (DSC), profilometry, Fourier transform infrared spectroscopy (FTIR) and scanning electron microscopy (SEM).

2. Materials and methods

2.1 Materials

The Ultimaker S3 from Ultimaker (Utrecht, the Netherlands); an FDM printer, was used to 3D print the PLA specimens. Ultimaker transparent PLA filament was used, acquired from Inspire3D (Rathnew, Co. Wicklow, Ireland). The filament had a diameter of 2.85 ± 0.10 mm and was extruded using the Ultimaker 0.4 AA print core. Injection moulded PLA specimens were produced at Smallwares Injection Moulding, Dundalk, Ireland, using TotalEnergies Corbion Luminy® L130 PLA. Physical and thermal properties have previously been detailed.[62]

'Living Green All-Purpose Compost' was purchased commercially. The contents of this compost were peat, worm-cast, and manure, as stated on the label. Compost was sieved through a 2 mm mesh prior to use and stored in sealed containers at room temperature (20 °C). Macherey-Nagel pH-fix pH indicator strips were purchased from Fisher Scientific.

2.2 Methods

2.2.1 PLA 3D printing and recycling. Onshape was used to design and sketch the PLA specimens. Ultimaker Cura software was used to 3D print the specimens. A print speed of 15 mm s^{-1}, a layer height of 0.04 mm and a print temperature of 200 °C were used as previously reported.[61] The 3D-printed specimens had a thickness of 1 mm, with 100% infill in a 'concentric' or 'zig zag' pattern as noted. 3D-printed dogbones had the dimensions shown in Fig. 1a. 3D-printed and injection moulded coupons had a diameter of 2 cm (Fig. 1b). PLA labware, both
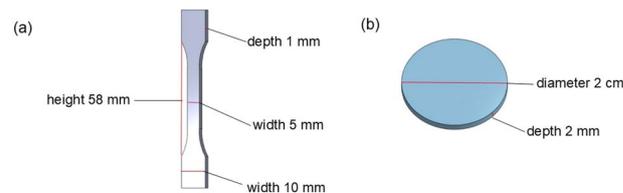

Fig. 1 Schematic of (a) dogbone dimensions and (b) coupons used in this study.

3D-printed and injection moulded had dimensions as previously described.[62]

To produce recycled PLA filaments (Fig. 2), Ultimaker transparent PLA filament was passed through a Filabot Reclaimer instrument, firstly through the shredder that breaks the long PLA filament into smaller pieces, and secondly through the granulator that further breaks down these pieces into smaller, extrudable size (~1 mm). Granules were washed and dried at 45 °C overnight to remove any moisture. These granules are then fed into a 3Devo filament maker one precision extruder. The extruder was operated at 60 rpm, with a temperature profile of 170 °C (hopper), 185 °C, 190 °C, and 195 °C (die). A fan solidified the molten PLA into a filament and when the extruded filament had reached a steady state of 2.85 mm + 0.10 mm, it was spooled into a reel. This recycled PLA filament was then 3D printed under the same conditions as outlined above. A portion of the recycled PLA filament was shredded into granules and the extrusion process repeated. The recycling process was repeated until loss of processability (i.e. PLA material was too brittle and could not be 3D printed) was reached.

PLA coupons, both 3D-printed and injection moulded, were subjected to the post-processing methods of autoclave sterilization. Conditions and equipment used for these sterilization techniques have previously been detailed.[61] The various PLA specimens and associated abbreviations used in the study are given in Table 1.

2.2.2 Composting conditions and maintenance. Moisture content of the compost was determined by weighing a sample (previously sieved through 2 × 2 mm mesh) to give the initial weight ($w_{initial}$). This sample was then placed in an oven at 105 °C until constant weight was achieved (w_{final}). The moisture content of the compost was then calculated using eqn (1). Moisture content was calculated to be 62 + 3%.

$$\frac{w_{initial} - w_{final}}{w_{initial}} \times 100 \quad (1)$$

For pH measurements, sieved compost samples were added to deionised water in a 1 : 2 w/v ratio and left at room temperature for 1 h. The supernatant was then pipetted onto pH strips to determine the pH of the compost. Initial compost was determined to be pH 7.

Polypropylene plastic boxes with sealed lids were used as the composting vessels. Sieved compost was placed in the vessels with a minimum of ~5 cm headspace between the compost and the lid. PLA specimens were placed within the compost, with
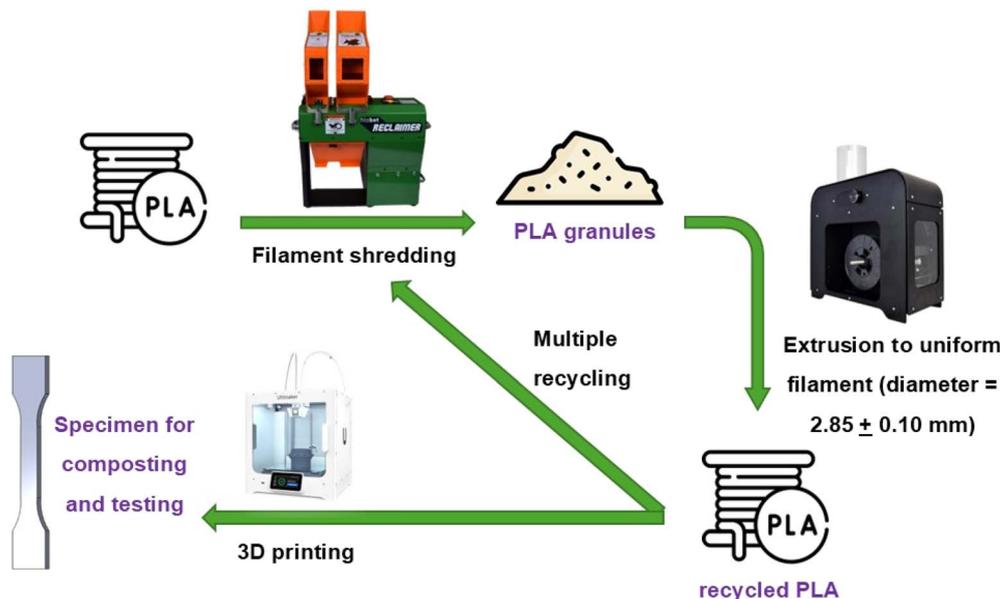
Fig. 2 Schematic of the mechanical recycling process.

a ratio of PLA material to compost at 2%. Composting vessels were placed in a Binder™ oven at a constant temperature of 58 °C. Vessels were incubated at the temperature for up to 12 weeks. Appropriate moisture levels and aeration of the compost was maintained following the schedule as described in ISO 20200:2023.[48] Three dogbone samples for the recycling PLA study were removed every week until disintegration of >90% was determined, in accordance with ISO 17088:2021, 'Specification for Compostable Plastics'.[64] Three PLA coupons were removed every week for the surface morphology study, up to five weeks.

2.2.3 Materials testing. Percentage disintegration of PLA specimens was determined by eqn (2).[65] An average mass was calculated of the various PLA specimens before composting (mass$_{week\ 0}$). When samples were collected every week during incubation, they were first washed with deionised water to remove compost particles. The samples were then placed in an

oven at 45 °C until constant weight and an average mass was obtained (mass$_{week\ X}$, $X =$ number of weeks composted). When PLA samples were disintegrated into multiple pieces, the compost was sieved through a 2×2 mm mesh to collect all pieces >2×2 mm in size.

$$\% \text{ Disintegration} = \frac{\text{mass}_{week\ 0} - \text{mass}_{week\ X}}{\text{mass}_{week\ 0}} \times 100 \qquad (2)$$

Tensile strength testing was performed on virgin PLA and recycled PLA specimens[66] both before and after composting, using a Zwick 5kn SB13 universal testing machine and a digiClip extensometer (Zwick Roell, Herefordshire, UK). For each sample category a minimum replicate of $N = 3$ was used with a grip distance (L) of 60 ± 0.5 mm, and a testing speed of 0.5 mm min^{-1} (2% of gauge length (L_0) min^{-1}). Ultimate tensile strength (MPa), maximum elongation (%), and Young's

Table 1 The PLA specimens produced for composting trials and associated abbreviations

12-week composting trial		5-week composting trial		4-week composting trial	
PLA specimen	Abbreviation	PLA specimen	Abbreviation	PLA specimen	Abbreviation
3D-printed Petri dish	3D_P	3D-printed, 'concentric' infill pattern coupon	3D_C	3D-printed dogbone	PLA
3D-printed 250 mL conical flask	3D_F	3D-printed, 'concentric' infill pattern coupon, autoclaved	3D_C_A	3D-printed, once recycled dogbone	Rec-1
Injection moulded Petri dish	IM_P	3D-printed, 'zig zag' infill pattern coupon	3D_Z	3D-printed, twice recycled dogbone	Rec-2
Injection moulded Petri dish, autoclaved	IM_P_A	3D-printed, 'zig zag' infill pattern coupon, autoclaved	3D_Z_A	3D-printed, three times recycled dogbone	Rec-3
		Injection moulded coupon	IM		
		Injection moulded coupon, autoclaved	IM_A		

modulus (MPa) data were obtained from the resulting stress *vs.* strain graphs.

Gel permeation chromatography (GPC, Agilent 1260Infinity II-MDS System) was used to determine the molecular weights and weight distributions of the PLA material after 3D printing or injection moulding.[67] The GPC was fitted with a guard column followed by two PLgel 5 μm MIXED-D 300 × 7.5 mm columns and simultaneously fitted with a refractive index detector (RID) and viscometer (VS). For system calibration, narrow linear PS standards for column calibration (EasiVial PS-M range of nominal Mp 162–400 000 Da) were used. Samples were dissolved in $CHCl_3$, 0.1% (w/v) and left overnight before being filtered over 0.22 μm nylon syringe filters prior to analysis. Measurements were taken at 30 °C, using $CHCl_3$ as the eluent with a flow rate of 1 mL min^{-1}. Agilent GPC/SEC software was used to carry out the analysis.

Differential scanning calorimetry (DSC 4000 System, Perki-nElmer) was used to determine the percentage crystallinity of the 3D-printed and injection moulded PLA material.[67] Samples (~10 mg) were enclosed in aluminium pans and crimped. The programming of all test samples followed the standard heating–cooling–heating cycle. In the first heating cycle, the samples were heated from −10 °C to 220 °C at a rate of 20 °C min^{-1} to erase any unwanted thermal history in the polymers during processing, which was followed by the cooling cycle down to −10 °C at the same rate. In the second heating cycle, the samples were then heated again from −10 °C to 220 °C at a rate of 20 °C min^{-1}. For the calculation of percentage crystallinity, eqn (3) was used where the data presented is collected from the second heating cycle only.

$$X_c = \frac{\Delta h_m - \Delta h_{cc}}{\Delta h_m^0} \times 100 \quad (3)$$

The specific enthalpy of melting (J g^{-1}, Δh_m) and specific enthalpy of cold crystallization (J g^{-1}, Δh_{cc}) were obtained from the second heating cycle. The theoretical enthalpy of melting of 100% crystalline PLA (Δh_m^0) is taken to be 93 J g^{-1}.[68,69]

FTIR spectra were obtained using a Thermo Scientific Nicolet iN10 MX Infrared Imaging Microscope with an ATR attach-ment.[67] The spectra were taken from 4000 to 500 cm^{-1}, with a resolution of 20 scans.

Surface roughness parameters of the PLA samples were determined using a Bruker ContourGT Profilometer. Objective magnification was set at ×5 and a FOV magnification lens of ×1 was used. The scan parameters were set at a speed of ×1, backscan of 50 μm, length of 50 μm, and a threshold of 0.1%. The VXI processing method was used.

Optical micrographs were obtained using a Keyence VHX-X1 3D digital microscope, VH-Z50 lens, using a magnification of ×100 or ×200.

SEM micrographs were obtained using a thermionic emis-sion Karl-Zeiss EVO LS15 scanning electron system with a LaB6 filament, after gold sputtering (HHV Scancoat Six).

2.2.4 Statistical analysis. Statistical analysis was performed for tensile strength data with OriginPro2023. Paired sample *t*-tests were carried out to determine significance differences

between means. The null hypothesis was set as no difference between virgin PLA 3D-printed dogbones and recycled PLA 3D-printed dogbones or virgin/recycled PLA 3D-printed dogbones that had been composted. Significance level was set at $p \leq 0.05$.

3. Results and discussion

3.1 Disintegration of 3D-printed and injection moulded PLA labware components

3D-printed and injection moulded PLA-based labware has previously been designed and produced by the authors.[61,62] To investigate the complete life cycle of the PLA-based labware, composting studies were carried out on the 3D-printed Petri dish (3D_P), 3D-printed 250 mL flask (3D_F), the injection moulded Petri dish (IM_P), as well as an autoclaved, injection moulded Petri dish (IM_P_A) (Fig. 3). An IM_P specimen was autoclaved at 121 °C, 15 psi, for 15 minutes to replicate the real-life end-of-life of biodegradable bioscience labware, as all lab-ware would need to be decontaminated after standard use. The labware did not undergo any alternative sterilization.

PLA is a biodegradable material, but only under elevated temperatures (>55 °C),[70,71] with material properties such as molecular weight, percentage crystallinity, and surface morphology affecting the rate of degradation. A 12-week ther-mophilic (58 °C) composting trial was conducted on the four labware pieces. The degree of disintegration of each of these labware pieces is given in Fig. 4.

3D_P and 3D_F had reached the standard as indicated in ISO 20200:2023, with greater than 90% of the material being di-sintegrated into <2 × 2 mm pieces after 12 weeks at 58 °C, using the commercially available compost purchased. IM_P was 54% disintegrated, while IM_P_A was 81% disintegrated. It is evident from various studies described in the literature that increased M_W and % crystallinity of PLA polymers will decrease the rate of disintegration.[34–38] From a previous study,[62] the 3D-printed and
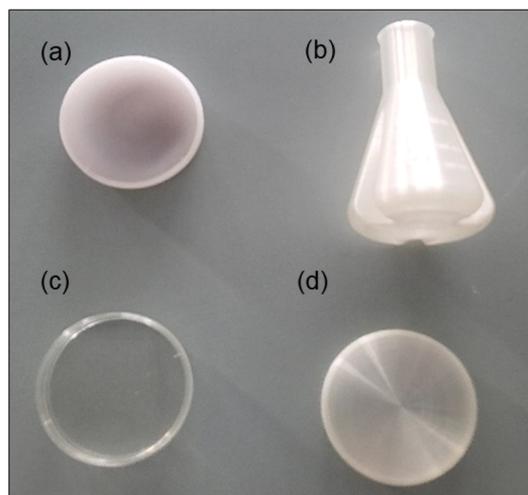

Fig. 3 PLA-based labware components for composting. (a) Auto-claved injection moulded Petri dish (IM_P_A), (b) 3D-printed 250 mL conical flask (3D_F), (c) injection moulded Petri dish (IM_P), (d) 3D-printed (3D_P) Petri dish.
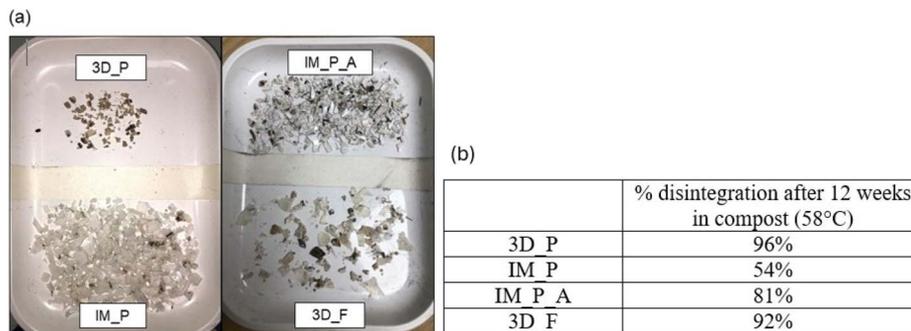
Fig. 4 (a) Disintegrated pieces of PLA-based labware >2 × 2 mm in size after sieving of compost after 12 weeks thermophilic composting. (b) % Disintegration of the four labware components.

IM labware had similar starting M_W (~150 kDa, Fig. 5c, week 0). It was postulated after this initial disintegration study that the internal polymer arrangement (*i.e.*, % crystallinity) could be leading to the difference of % disintegration between the 3D-printed labware (>90%) and the IM labware (54%). The increased % disintegration of IM-P_A (81%) compared to IM_P was expected, as it has been indicated that the autoclaving process decreases M_W of PLA polymers, which will lead to faster disintegration.[27,63] The thermal properties, % crystallinity, and M_W of the PLA materials before and after the composting trial were therefore next determined (Fig. 5).

The glass transition temperature (T_g) of 3D-printed PLA components decreased from 62.43 °C to 51.05 and 57.46 °C for the 3D_P and 3D_F respectively after the 12-week period. A
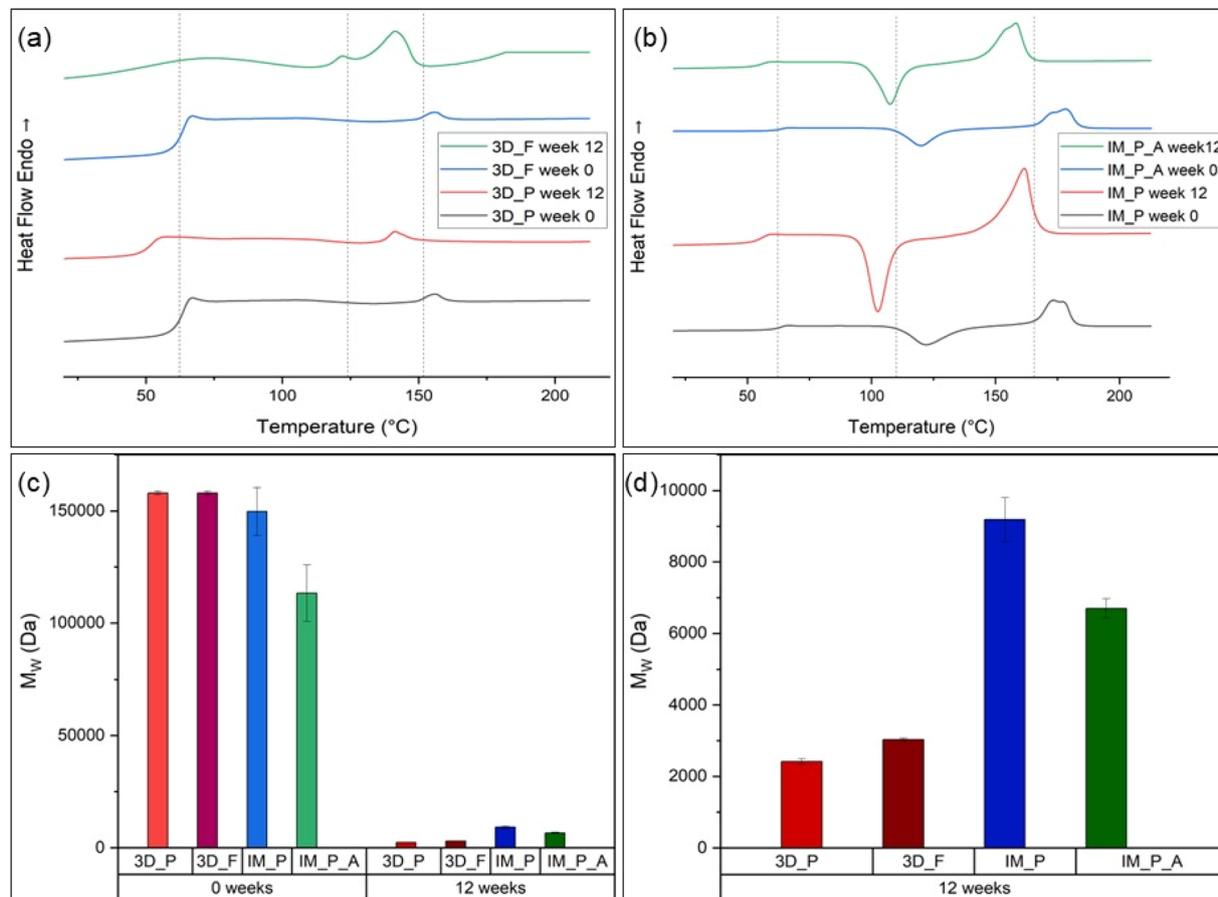

Fig. 5 (a) DSC thermographs of 3D_P and 3D_F before (week 0) and after (week 12) composting. (b) DSC thermographs of IM_P and IM_P_A before (week 0) and after (week 12) composting. Dashed lines indicate the thermal transition temperatures of 3D or IM PLA material before composting trials. (c) Weight average molecular weights (M_W, Da) PLA specimens before (week 0) and after (week 12) composting. (d) Zoomed in graph of M_W (Da) of the PLA specimens after composting (week 12).

Table 2 The thermal transitions of the four PLA labware components and enthalpies of cold crystallization and melting

0 weeks	3D_P	IM_P	IM_P_A	3D_F
T_g (°C)	62.43 + 1.89	62.39 + 0.19	63.01 + 0.28	62.43 + 1.89
T_{cc} (°C)	124.08 + 2.01	110.17 + 0.16	107.75 + 0.01	124.08 + 2.01
ΔH_{cc} (J g^{-1})	−0.34 + 0.12	−38.94 + 1.74	−43.01 + 1.61	−0.34 + 0.12
T_m (°C)	153.92 + 1.78	165.72 + 0.10	165.12 + 0.08	153.92 + 1.78
ΔH_m (J g^{-1})	0.75 + 0.34	43.26 + 1.17	43.64 + 1.53	0.75 + 0.34
After 12 weeks	3D_P	IM_P	IM_P_A	3D_F
T_g (°C)	51.05 + 2.01	54.33 + 1.87	55.68 + 0.31	57.46 + 2.56
T_{cc} (°C)	107.83 + 2.91	93.70 + 2.89	97.54 + 0.56	78.61 + 1.45
ΔH_{cc} (J g^{-1})	−1.28 + 0.47	−47.81 + 3.78	−46.13 + 0.33	−3.34 + 0.89
T_m (°C)	135.04 + 0.98	143.38 + 0.89	143.73 + 0.71	117.80 + 1.10
ΔH_m (J g^{-1})	2.99 + 1.45	59.93 + 3.79	54.64 + 2.11	68.78 + 3.45

similar decrease in cold crystallization temperature (T_{cc}) and melting temperature (T_m) after the 12 weeks of thermophilic composting was observed. IM_P and IM_P_A also showed a decrease in thermal transitions after 12 weeks of composting (Table 2). The decrease in thermal transition temperatures is due to the hydrolytic cleavage of the polymer chains, resulting in lower M_W chains that have greater mobility and require less energy (*i.e.*, lower temperatures) to rearranged during glass

transitions, crystallization and melting.[37,72] This pattern of decreasing thermal transition temperatures aligns with the decrease in M_W after 12-week composting observed for all four PLA labware components. The % crystallinities of all PLA materials were calculated (Table S1). 3D-printed PLA materials showed % crystallinities below 1%. IM_P had a % crystallinity of 4.7%, while after autoclaving the resulting material, IM_P_A, had a % crystallinity of 1.3%. The autoclaving process therefore
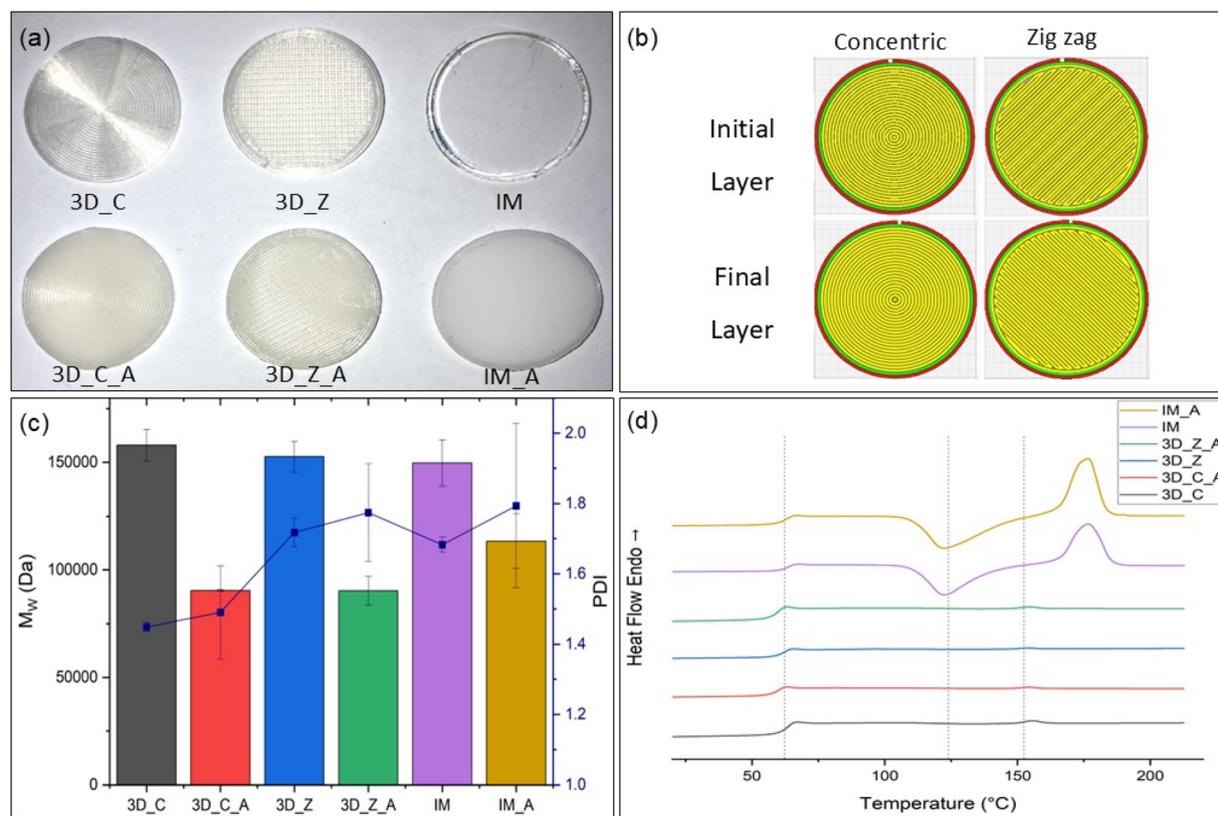

Fig. 6 (a) Images of 2 cm PLA coupons. (b) Schematic of the 'concentric' *vs.* 'zig zag' infill patterns used to produce the 3D-printed PLA coupons. (c) Weight average molecular weights (M_W, Da) (bars) and polydispersity index (line) of PLA coupons. (d) DSC thermographs of PLA coupons. Dashed lines indicate the thermal transition temperatures of 3D-printed PLA coupons before composting trials.

led to a rearrangement of the polymer chains, increasing the amorphous regions in the PLA material.[73]

Weight average molecular weights (M_W, Da) of the PLA materials before and after 12 weeks composting is given in Fig. 5c and d, as determined by GPC analysis. The M_W of the 3D-printed labware PLA had decreased by 98%, while the M_W of IM specimens had both decreased by 94%. All the labware therefore had a significant decrease in the M_W of the PLA polymers, though this did not equate to levels of disintegration. To understand the impact of surface morphology, molecular weight, and % crystallinity on the disintegration rate of PLA, a five-week thermophilic composting study was undertaken.

3.2 Five-week disintegration trial of PLA coupons

PLA coupons 2 cm in diameter were 3D printed or laser cut from the injection moulded Petri dish (IM). All coupons were 1 cm

thick (Fig. 6a). PLA coupons were printed in either the 'concentric' infill pattern (3D_C), identical to the Petri dish and flask pattern, or the 'zig zag' infill pattern (3D_Z) (Fig. 6b). The different Ultimaker Cura infill patterns were chosen to investigate the effect of surface morphology on PLA disintegration, while keeping the molecular weight and % crystallinity parameters constant. All three PLA coupon specimens were autoclaved at 121 °C, 15 psi for 15 minutes. Micrographs of the six PLA coupon specimens are given in Fig. S1 in the SI. The initial M_W and thermal transitions of the resulting six PLA coupon specimens are given in Fig. 6c and d. Autoclaving under the conditions given decreased the M_W of the 3D-printed coupons by 41–43% (3D_Z_A and 3D_C_A) and the injection moulded coupon by 24%. The thermal transitions of all coupons were not significantly altered following autoclaving, although the % crystallinity decreased from 4.7% (IM) to 1.8% (IM_A) for the injection moulded coupons (Table S1). The
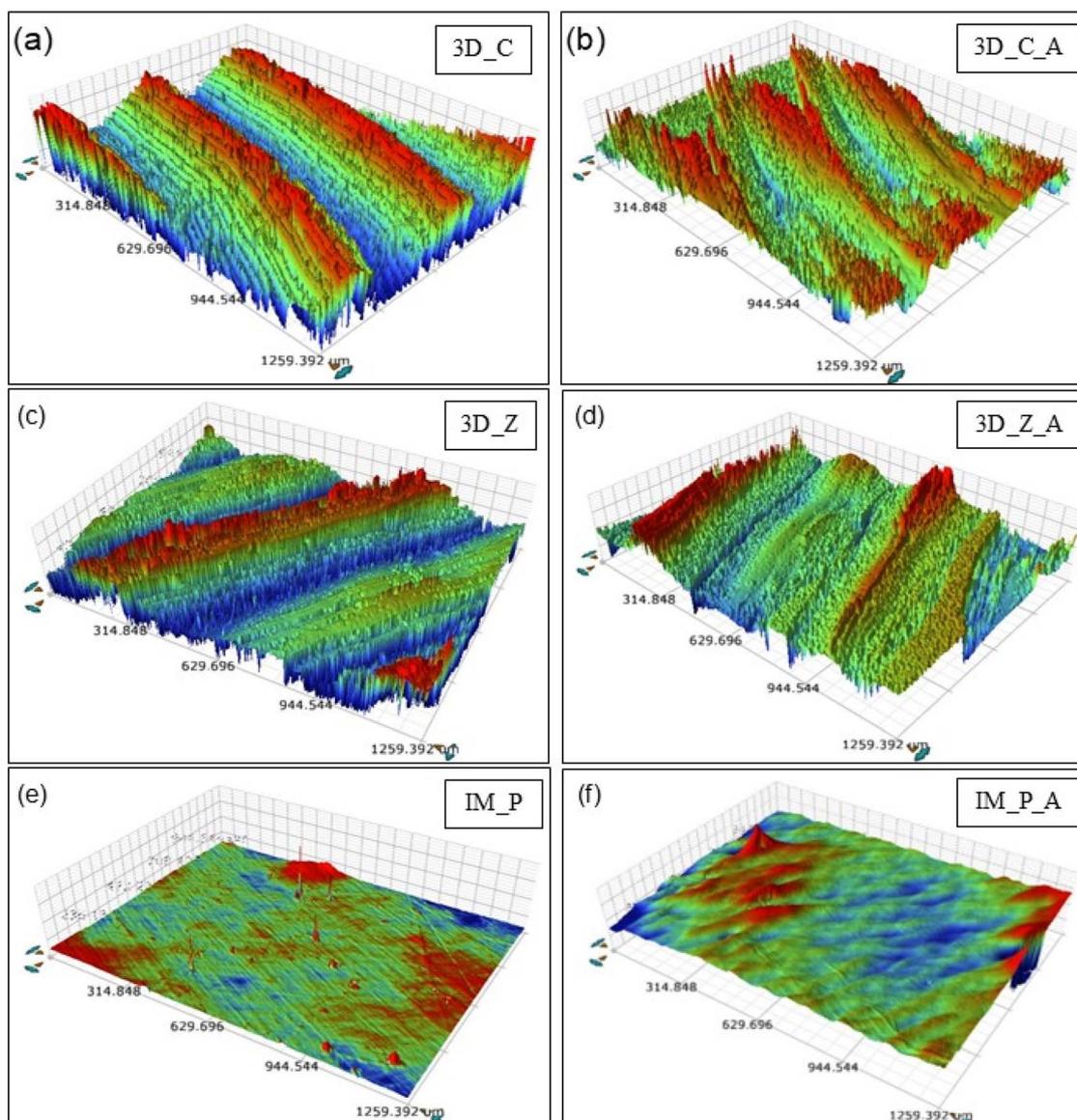

Fig. 7 Surface profiles of 3D-printed and injection moulded PLA coupons. (a) 3D_C, (b) 3D_C_A, (c) 3D_Z, (d) 3D_Z_A, (e) IM, (f) IM_A.

Table 3 Surface analysis of PLA coupons

	3D_C	3D_C_A	3D_Z	3D_Z_A	IM	IM_A
S_a (μm, areal roughness)	10.942 + 1.185	11.964 + 0.730	8.454 + 0.763	9.422 + 0.246	0.024 + 0.001	0.172 + 0.008
S_q (μm, root mean square areal roughness)	13.199 + 2.060	14.860 + 0.676	11.079 + 1.365	12.409 + 0.395	0.064 + 0.020	0.2435 + 0.011
S_p (μm, max. peak height)	43.192 + 18.769	49.054 + 6.452	48.584 + 4.376	47.364 + 2.732	3.892 + 0.826	3.247 + 1.527
S_v (μm, max. pit depth)	−34.972 + 7.676	−46.877 + 3.381	−40.178 + 3.554	−47.618 + 0.821	−0.302 + 0.059	−3.563 + 1.120
S_z (μm, max. height difference)	78.255 + 6.316	95.931 + 9.833	88.757 + 7.937	94.981 + 1.911	4.194 + 0.767	6.809 + 2.727

autoclaving process therefore led to a rearrangement of the polymer chains, increasing the amorphous regions in the PLA material.[73] This could be due to hydration of the PLA material, which has been shown to have a significant effect on PLA structure due to strong intermolecular interactions between water molecules and PLA polymer chains.[74]

The surface roughness of the PLA coupons prior to composting was determined using interferometry. The results are given in Fig. 7 and Table 3.

The areal surface roughness (S_a) is slightly higher for 3D_C (10.942 + 1.185 μm) compared to 3D_Z (8.454 + 0.763 μm)

coupons, due to the printing infill pattern. 'Concentric' printing pattern results in the filament (0.4 mm width) being deposited in the same orientation every layer. 'Zig zag' infill pattern deposits the filament in a diagonal orientation, shifting the orientation by 90° for every layer. The difference in S_a for the 3D-printed coupons (3D_C and 3D_Z) compared to IM coupons (0.024 + 0.001 μm) is significant, as expected.[75,76] Autoclaving led to an increase in areal surface roughness for all PLA coupons. The process of autoclaving, where the temperature reaches 121 °C, leads to significant rearrangement of the polymer chains, as the temperature surpasses 60 °C (approximate T_g of
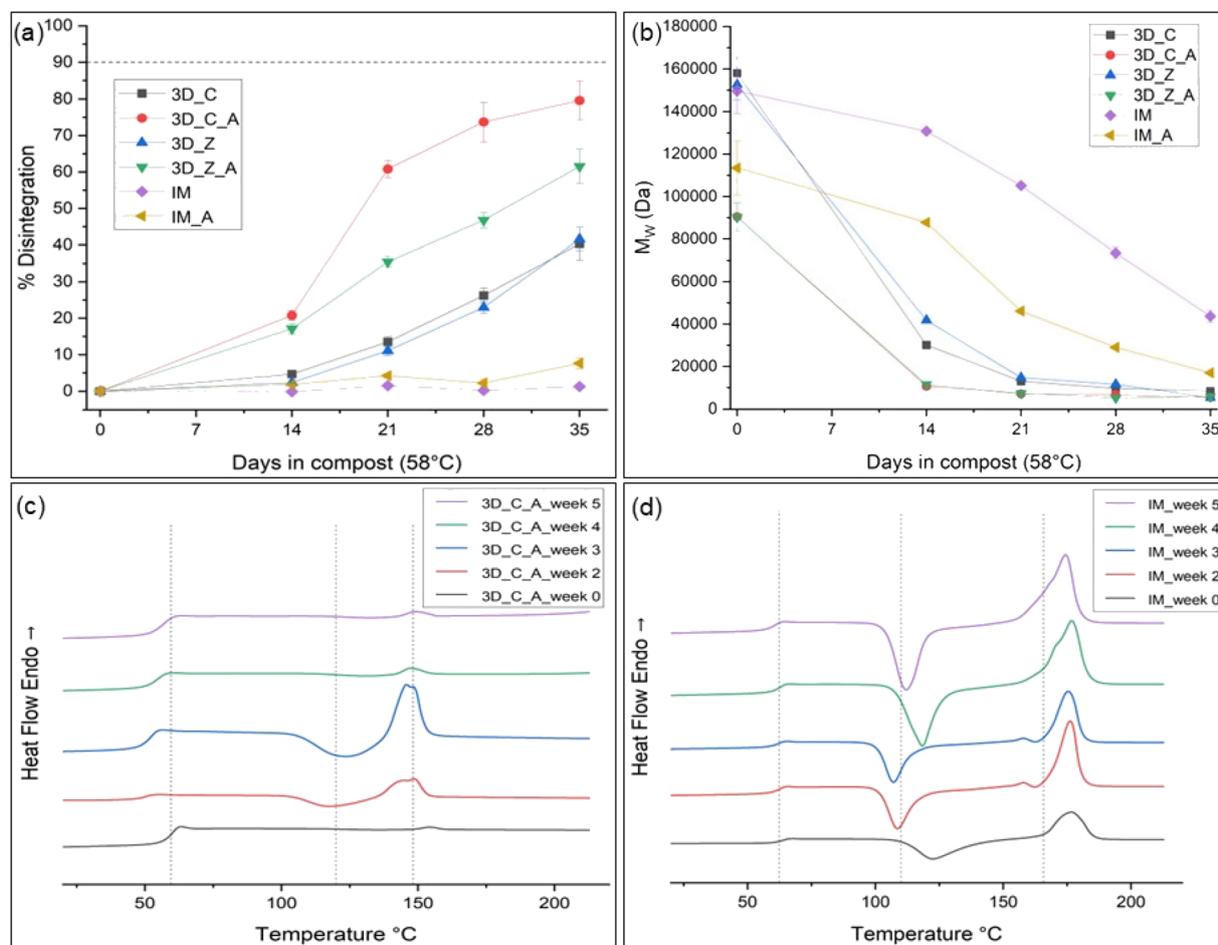

Fig. 8 (a) % Disintegration of PLA coupons during five-week composting trial. (b) Weight average molecular weights (M_W, Da) of PLA coupons during composting. (c) DSC thermographs of 3D_C_A PLA coupons during composting. (d) DSC thermographs of IM PLA coupons during composting. Dashed lines indicate the thermal transition temperatures of PLA coupons before composting trials (week 0).

PLA) and 120 °C (approximate T_{cc} of PLA). The humid environment of the autoclave also leads to hydrolysis of the PLA polymer chains in the amorphous region,[25] as shown in the decreased M_W for the autoclaved coupons. Increased S_a of 3D-printed coupons compared to injection moulded coupons can result in increased surface area where hydrolysis can occur, resulting in the decreased M_W for 3D_C_A and 3D_Z_A, compared to IM_A (Fig. 6c).

The six coupon samples were placed in compost under the same conditions as described for the PLA-based labware. The % disintegration for each sample was determined between 2–5 weeks at thermophilic composting conditions (Fig. 8a). IM showed no significant % disintegration within the 35 days of testing. This is in contrast with a recent study comparing the disintegration under industrial composting conditions on PLA and PLA–rosin resin composites.[66] In this study, mass loss of the neat PLA began by day 21 and by day 35 the disintegration was >20%. The samples tested in the study were of the dimensions $25 \times 25 \times 1$ mm³. This could indicate the importance of initial product dimensions on disintegration rate. The initial molecular weight of the neat PLA was not included in this study. The % crystallization of the neat PLA was determined to be 6.3%, while the IM PLA used in this study showed a % crystallization of 4.7%. The rate of disintegration was increased for the autoclaved 3D-printed PLA coupons (3D_C_A and 3D_Z_A) compared to the 3D printed PLA coupons that were not autoclaved before composting (3D_C and 3D_Z). In particular, 3D_C_A showed the greatest rate of disintegration, reaching 80% disintegration after 5 weeks. It must be noted that after

four weeks of composting, the autoclaved PLA coupons, 3D_C_A and 3D_Z_A, had disintegrated to such an extent that it was necessary to piece together the coupons from the compost, disregarding all PLA pieces $<2 \times 2$ mm. Therefore, there is potential human error in the % disintegration calculation for the week 4 autoclaved coupons, as represented in the greater standard deviation for these values.

The increased surface area of 3D_C_A compared to the other PLA coupon samples may lead to the increased rate of disintegration observed. The M_W of 3D_C_A and 3D_Z_A are statistically the same prior to composting and the M_W of both decreased at a similar rate during the five-week composting trial (Fig. 8b). After week 3 under thermophilic composting conditions, all the 3D-printed PLA coupons had M_W in the range 7–14 kDa and the rate of decrease in M_W had plateaued. By comparison, IM coupons had a M_W of 105 kDa at week 3 and this had decreased to 44 kDa by the end of the trial at week 5. The IM and IM_A samples showed the slowest rate of disintegration during the five-week trial, possibly due to the relatively smooth surface compared to the 3D-printed PLA coupons. This loss of M_W during the first 30–60 days is due to hydrolysis rather than enzymatic biodegradation, as determined by a recent study where a full biodegradation analysis of stereocomplex PLLA/PDLA materials was investigated.[77] The sudden reduction in M_W after 14 days in compost, similar to the behaviour observed here for all of the 3D-printed coupons, has been mathematically modelled[78] and has been attributed to the dissolution of the oligomer intermediates and the autocatalytic action of the PLA oligomers once degradation has begun.
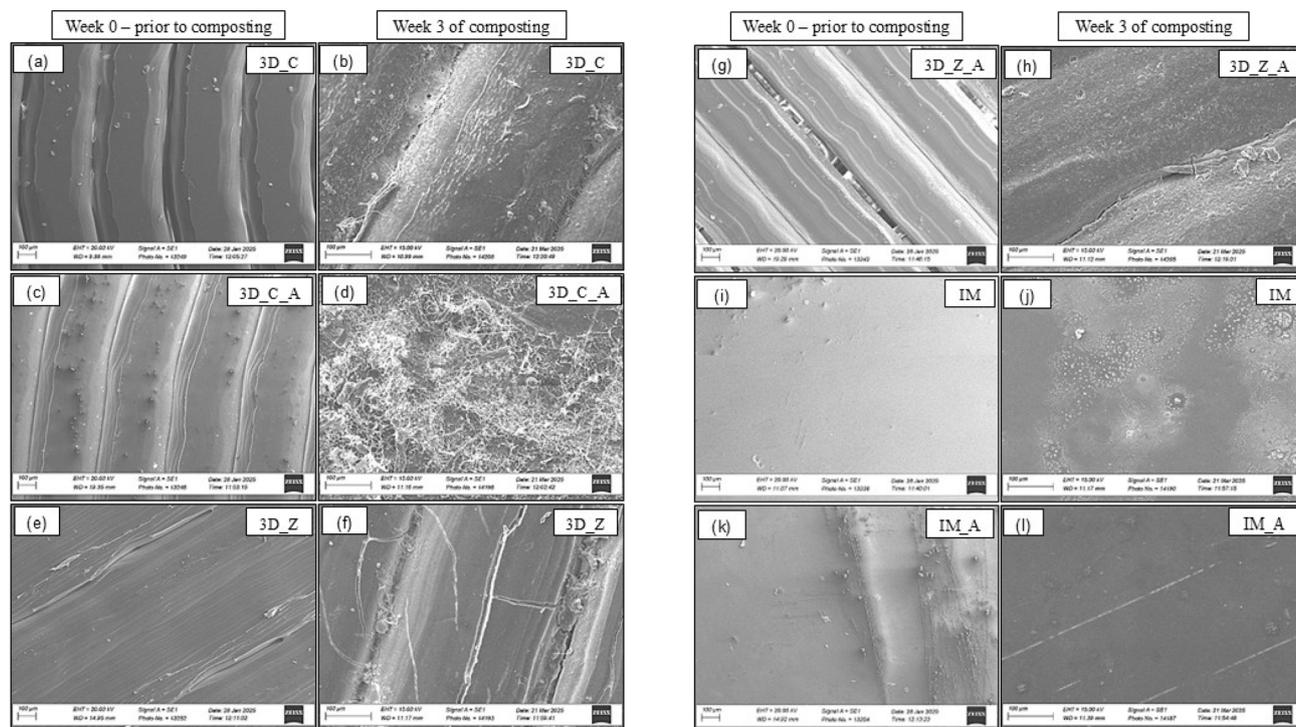

Fig. 9 SEM micrographs of PLA coupons. (a) 3D_C_week 0, (b) 3D_C_week 3, (c) 3D_C_A_week 0, (d) 3D_C_A_week 3, (e) 3D_Z_week 0, (f) 3D_Z_week 3, (g) 3D_Z_A_week 0, (h) 3D_Z_A_week 3, (i) IM_week 0, (j) IM_week 3, (k) IM_A_week 0, (l) IM_A_week 3.

Thermographs of 3D_C_A and IM are given in Fig. 8c and d respectively. This further exemplifies the increased rate of degradation of the PLA polymer chains for 3D_C_A compared to IM. The thermal transitions of 3D_C_A occur at lower temperatures within the first 2 weeks of thermophilic composting compared to IM. For example, the T_m of 3D_C_A had decreased from 148.24 °C (week 0) to 136.56 °C (week 2), while the T_m of IM had decreased from 165.72 °C (week 0) to 164.69 °C (week 2). This is in contrast with a recent study that showed T_m to decrease by approximately the same degree of amorphous PLA film (thickness = 195 μm) and 20% crystalline PLA film (thickness = 215 μm) over a two week composting period.[33] This could point to the importance of the external surface area of PLA over internal polymer orientation during the initial phase of disintegration. Furthermore, it has been shown that the % crystallization of PLA increases at 58 °C after a prolonged period of time.[79] This is evidenced here, where 3D_C_A was 0.3% crystalline at week 0 but had increased to 1.9% at week 2 of composting. IM had a starting crystallinity of 4.7% at week

0 and this had increased to 12.8% by week 2 of composting. This increase in crystallinity could slow down PLA degradation in the compost, especially for the IM coupon, leading to the much slower rate of disintegration (Fig. 8a). Thermographs for 3D_C, 3D_Z, 3D_Z_A, and IM_A can be found in Fig. S2 and thermal transition data can be found in Table S2.

SEM analysis of PLA coupons prior to composting (week 0) and after composting for 3 weeks (Fig. 9) was conducted. The SEM micrographs showed visible porosity of the PLA coupons after 3 weeks of thermophilic composting for the 3D-printed coupons. Pore formation in PLA under aqueous and composting conditions have been reported,[80,81] due to the solubilization of the oligomers following the decrease in M_W of the polymer chains and water sorption. It has been shown that oligomers formed during composting as present at the sample surface of a fully amorphous PLA injection moulded material, while the oligomers formed from a more crystalline injection moulded material are located within the polymer matrix.[82] The authors postulate that the denser structure of the crystalline material
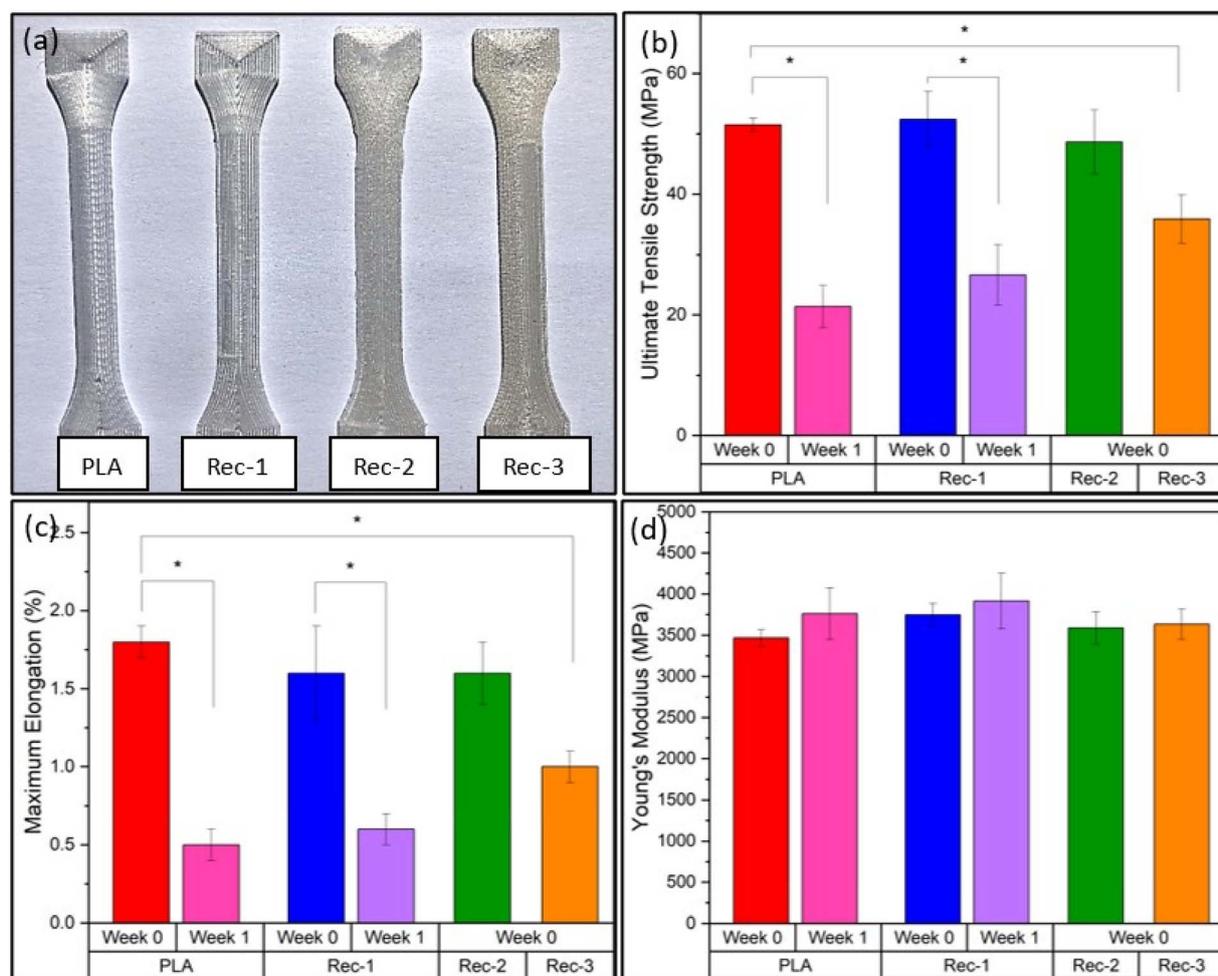

Fig. 10 (a) Images of 3D-printed dogbones. (b) Ultimate tensile strength (MPa) of 3D-printed dogbone specimens prior to composting (week 0) and after 1 week of composting. (c) Maximum elongation (%) of 3D-printed dogbone specimens prior to composting (week 0) and after 1 week of composting. (d) Young's modulus (MPa) of 3D-printed dogbone specimens prior to composting (week 0) and after 1 week of composting. * = statistically significant difference, $p < 0.05$.

prevents the oligomers from diffusing through the material as readily as if they are on the surface. This leads to a slower degradation process and slower reduction in M_W of the crystalline material. When comparing disintegration of 3D-printed *vs.* injection moulded PLA coupons as in the work, the denser structure of the PLA for IM and IM_A may be preventing oligomers that are forming through hydrolytic cleavage from diffusing through the material and being released into the compost. This may be the cause of the steadily decreasing M_W of IM and IM_A (Fig. 8b) but with no apparent decrease in the overall mass loss (Fig. 8a). Much focus has been given in the literature to the effect of amorphous *vs.* crystalline PLA sample degradation under various conditions.[25,83,84] This work aims to advance the knowledge of PLA degradation behaviour by investigating the initial disintegration of PLA samples with altered surface topography, while keeping initial M_w and crystalline properties relatively consistent. The altered surface topography of the PLA specimens has a marked impact on initial disintegration under industrial composting conditions. This is therefore an important aspect to consider when developing PLA-based products for real-world applications.

3.3 Disintegration trial of recycled PLA dogbones

The final aspect of this study investigated the impact of mechanical recycling on the disintegration of 3D-printed PLA under thermophilic composting conditions. The mechanical recycling process as outlined in Fig. 2 allowed the Ultimaker Cura PLA filament to be recycled up to three times. During the fourth recycling round, the extruded filament became too brittle to process through the 3D printer. The effect of mechanical recycling on PLA for 3D printing has been investigated[52,85–87] and this finding of the limitation of recycling for PLA is consistent with what has been reported previously. The non-recycled PLA dogbones and once, twice, and three-times (Rec-1, Rec-2, Rec-3) recycled PLA dogbones were composted in identical conditions as described previously. The mechanical properties of the dogbones prior to and during composting were investigated (Fig. 10). The values for PLA dogbones are in agreement with those in the literature.[66] There was no significant change in the ultimate tensile strength (MPa) of the PLA dogbones after the first and second round of recycling. However, Rec-3 dogbones showed a significant reduction in ultimate tensile strength
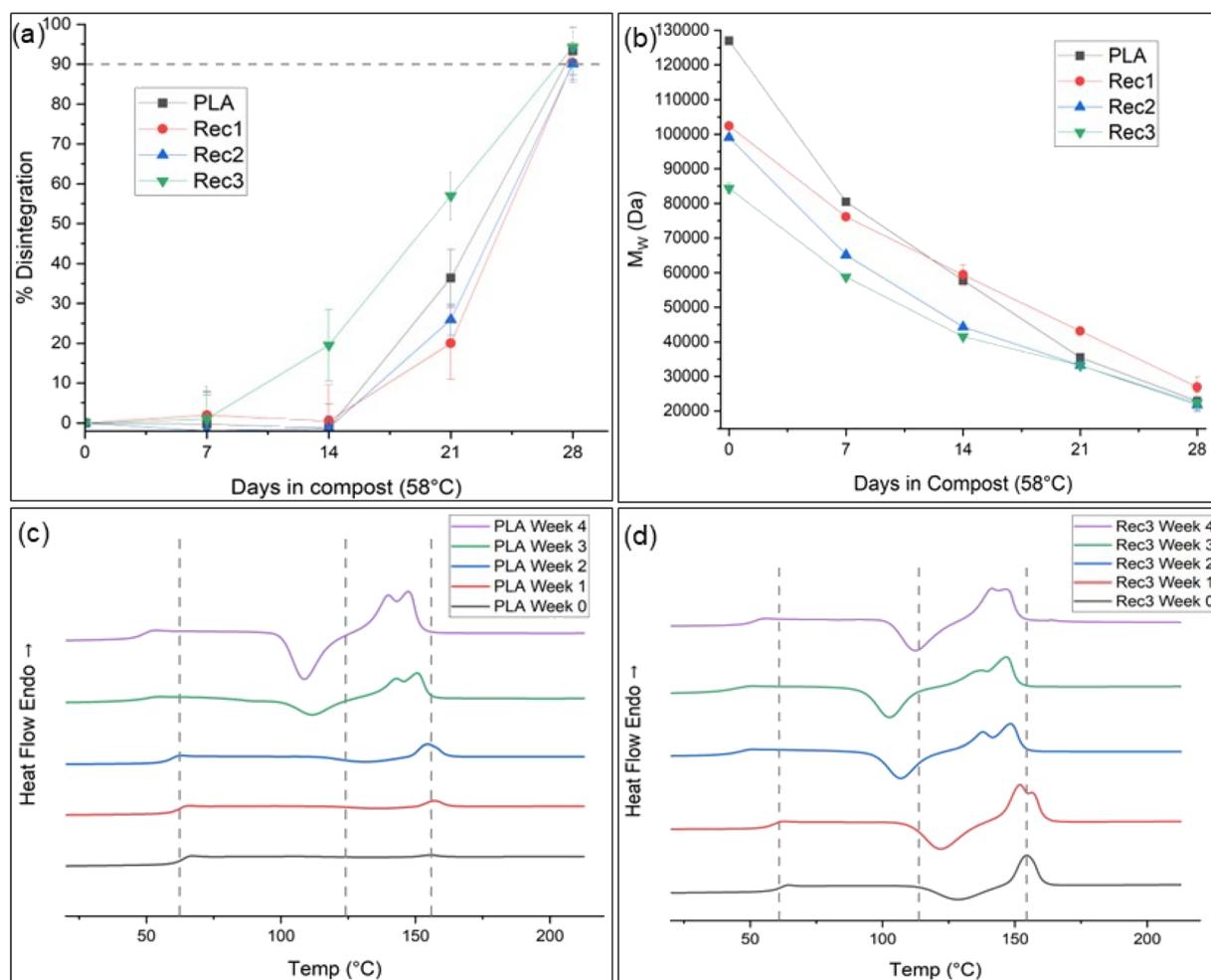

Fig. 11 (a) % Disintegration of 3D-printed dogbones during four-week composting trial. (b) Weight average molecular weights (M_W, Da) of 3D-printed dogbones during composting. (c) DSC thermographs of 3D-printed PLA dogbones during composting. (d) DSC thermographs of 3D-printed Rec-3 dogbones. Dashed lines indicate the thermal transition temperatures of 3D-printed dogbones before composting trials (week 0).

compared to PLA dogbones, from 51.51 + 1.10 to 35.90 + 3.99. After one week of thermophilic composting, the tensile strength of the PLA and Rec-1 dogbones had decreased significantly and the Rec-2 and Rec-3 dogbones were too brittle to obtain reliable results. The maximum elongation measurements followed the same pattern, with a significant difference between PLA and Rec-3 dogbones prior to composting and a significant reduction in maximum elongation after one week of composting for all dogbone specimens. The Young's modulus, a measure of the elasticity of the material, remained unchanged following the recycling rounds and after one week of composting. Data can be found in Table S3.

The % disintegration of the dogbone specimens were calculated during composting for four weeks after which all the specimens had reached ≥90% disintegration (Fig. 11a). The rate of disintegration did not change when comparing Rec-1 and Rec-2 dogbones to PLA dogbones. Rec-3 dogbones showed an increased rate of disintegration, though after four weeks in thermophilic composting conditions all dogbone specimens were 90–94% disintegrated. Rec-3 was 20% disintegrated after two weeks thermophilic composting, while PLA, Rec-1, and Rec-2 showed no weight loss. The initial M_W prior to composting for Rec-3 was 84 kDa, while Rec-1 and Rec-2 dogbones were in the range 99–102 kDa, and virgin PLA was 130 kDa (Fig. 11b). All dogbone specimens M_W were in the range 22–26 kDa after four weeks composting, consistent with the finding that all dogbones had reached ≥90% disintegration at this stage of composting. Thermal analysis showed that with increasing rounds of mechanical recycling, the thermal transitions all began to decrease earlier in the composting process. This is to be expected, as decreasing M_W leads to lower thermal transition temperatures.[88] Fig. 11c and d show thermographs of PLA and Rec-3 dogbones during the four-week composting trial. The remaining thermographs and corresponding data can be found in Fig. S3 and Table S4. The 3D-printed dogbones were analysed using ATR-FTIR to determine if any change in the chemical bonds of the polymer chains could be observed during the composting process. No noticeable changes were detected in the resulting spectra (700–3700 cm^{-1}). This is in agreement with a recent study that showed no substantial change in the chemical composition of PLA foils, as investigated by FTIR spectroscopy.[89] The authors noted a broad band appearing in the region of 3100–3300 cm^{-1}, attributed to biofilm formation. This was not observed for the PLA dogbones and could be due to the microbial make-up of the compost itself. The spectra can be found in Fig. S4.

The 3D-printed dogbones were visualized under an optical microscope. The alterations in surface composition of the non-recycled vs. recycled PLA dogbones and the dogbones prior to composting (week 0) vs. dogbones after 3 weeks composting is given in Fig. 12. After three weeks of composting, the 3D-printed material showed the formation of pores on the surface, which became more evident with increased rounds of mechanical recycling. This could be due to the lower M_W of the polymer chains because of the repeated heat cycles during mechanical recycling. The shorter polymer chains within the material can allow for the increased sorption of water onto the surface,
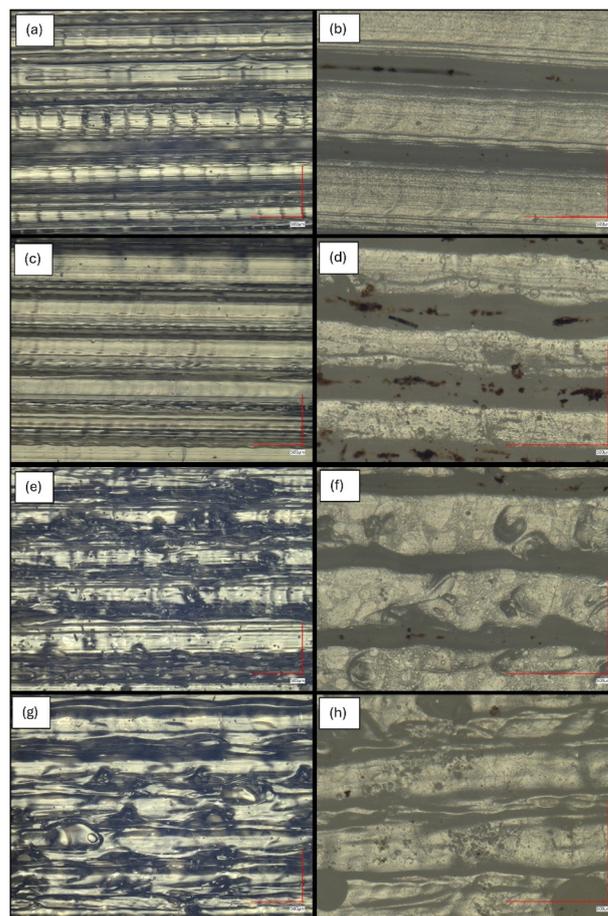

Fig. 12 Optical micrographs of 3D-printed dogbones. Red line indicates 500 μm. (a) PLA_week 0, (b) PLA_week 3, (c) Rec-1_week 0, (d) Rec-1_week 3, (e) Rec-2_week 0, (f) Rec-2_week 3, (g) Rec-3_week 0, (h) Rec-3_week 3.

leading to hydrolysis at these sites, resulting in the observed pores.[90]

From this study, it can be concluded that PLA can be mechanically recycled for up two rounds without any significant loss of mechanical strength and the disintegration of the material under industrial composting conditions was not altered. When the material was recycled for a third time, there was a significant reduction in tensile strength, and the rate of disintegration increased under industrial composting conditions. This finding advances the current knowledge of the degradation of 3D-printed recycled PLA specimens, as the degradation studies of recycled PLA cited in the literature focus on one round of mechanical recycling only and use PLA films as the end specimen.[91] The films investigated in that particular study had a thickness of 210 μm, and thus are disintegrated (>90%) by 21 days in compost.

4. Conclusion

In this study, PLA-based labware was produced through 3D printing or injection moulding and the disintegration of these components was studied under industrial composting

conditions according to ISO 20200:2023. An injection moulded Petri dish was autoclaved prior to the composting trial, to replicate the real-world application of bioscience labware which would require sterilization prior to composting. It was determined that the 3D-printed Petri dish and 3D-printed 250 mL conical flask reached >90% disintegration within the 12-week period. The injection moulded Petri dishes, both non-autoclaved (IM_P) and autoclaved (IM_P_A), did not reach this standard, with IM_P reaching 54% and IM_P_A reaching 81% disintegration after 12 weeks. The M_W of the PLA polymer chains had decreased by 98% and 94% for the 3D-printed and injection moulded labware respectively, as determined by GPC analysis. To further investigate the impact of surface topography vs. internal morphology on the disintegration rate of PLA, an in-depth 5-week composting trial was conducted on PLA coupons.

Six samples of PLA coupons were produced, two injection moulded (IM and IM_A), two 3D-printed with a 'concentric' infill pattern (3D_C and 3D_C_A), and two 3D-printed with a 'zig zag' infill pattern (3D_Z and 3D_Z_A). The different infill patterns were chosen to determine if altering the print pattern will lead to a change in the surface roughness and hence a change in the disintegration rate of the coupons, while keeping the M_W of the PLA coupons consistent. Autoclaving the PLA coupons led to an increase in surface roughness (S_a, μm) for all three PLA coupons, as determined by white light interferometry. It also led to a decrease in M_W, with a 41–43% decrease for the 3D-printed coupons and a 24% decrease for the injection moulded coupon. After 5 weeks of composting under thermophilic conditions, IM coupons had only reached 1.3% disintegration, although the M_W had decreased from ∼150 kD to ∼44 kDa. 3D_C_A coupons showed the greatest level of disintegration, at 79.6%. The 3D_C coupons had a 40.3% disintegration level at this stage, although the M_W of the coupons were in a similar range, between 5–8 kDa. The PLA materials used for the production of 3D-printed and injection moulded specimen has similar M_W prior to autoclaving and/or composting, and all had low crystallinity (<5%). These properties have been thoroughly investigated in relation to their impact on PLA degradation. This study highlights the impact of surface topography of biodegradable plastics such as PLA on disintegration rates during composting. The processing (3D-printed vs. injection moulded) and post-processing (autoclaved) methods altered the disintegration of the PLA material substantially. This variance in the disintegration of PLA based on surface topography should be considered when producing 'biodegradable' PLA products, and methods to increase surface roughness and/or hydrophilicity must be investigated.

Lastly, the impact of mechanical recycling of PLA on the disintegration rates under industrial composting conditions was investigated. PLA was mechanically recycled up to three times. There was a significant reduction in tensile strength (MPa) of the material after the third round of recycling. The dogbones produced from three times recycled PLA (Rec-3) showed an increased rate of disintegration, though all dogbones had reached ≥90% disintegration after 4 weeks. All dogbone specimens had reached a M_W of 22–27 kDa after 4

weeks of composting. This likewise highlights the impact of surface topography and structural integrity on composting rates, which should be considered when designing and producing products that will reach the standard of 'biodegradability', as outlined in international standards.

This research details the initial investigation into the overall biodegradation of PLA bioscience labware produced through two standard manufacturing techniques, 3D printing and injection moulding. Disintegration is the first step in this biodegradation process. To fully understand the biodegradability of the PLA-based labware, future studies will include investigating the CO_2 emission rate during composting and analysis of the PLA by-products released into the compost. The 3D-printed, injection moulded, and recycled PLA material will be compared using these parameters. Further biodegradation studies will be conducted using bioaugmented compost containing known PLA-degrading bacterial strains, for a more targeted degradation study of the PLA materials. Lastly, composting trials will be conducted on the PLA materials in various environments, e.g., at home composting conditions, (mesophilic, 20–45 °C), to determine if the 3D-printed and recycled PLA materials can reach the 'biodegradable' limit in this milder condition.

Author contributions

Jennie O'Loughlin – methodology, formal analysis, investigation, data curation, visualization, writing – original draft. Hannah McDonnell – investigation, data curation. Robyn Lawless – investigation, data curation. Susan M. Kelleher – funding acquisition. Samantha Fahy – funding acquisition. Brain Freeland – funding acquisition. Keith D. Rochfort – funding acquisition, writing – review and editing. Jennifer Gaughran – supervision, funding acquisition, writing – review and editing.

Conflicts of interest

The authors declare that they have no known competing financial interests or personal relationships that influenced the work reported in this paper.

Data availability

The data supporting this article have been included as part of the supplementary information (SI). Supplementary information is available. See DOI: **https://doi.org/10.1039/d5su00623f**.

Acknowledgements

References

1 Global Plastic Production, https://www.statista.com/statistics/282732/global-production-of-plastics-since-1950/, accessed 7 January 2025.

2 Bioplastics Market Development Update, https://www.european-bioplastics.org/bioplastics-market-development-update-2023-2/, accessed 11 March 2024.

3 Plastics – the fast Facts 2023 Plastics Europe, https://plasticseurope.org/knowledge-hub/plastics-the-fast-facts-2023/, accessed 7 January 2025.

4 N. Singh and T. R. Walker, *Npj Mater. Sustain.*, 2024, **2**, 1–7.

5 I. A. Lakhiar, H. Yan, J. Zhang, G. Wang, S. Deng, R. Bao, C. Zhang, T. N. Syed, B. Wang, R. Zhou and X. Wang, *Agronomy*, 2024, **14**, 548.

6 F. Haq, M. Kiran, I. A. Khan, S. Mehmood, T. Aziz and M. Haroon, *Mater. Today Sustain.*, 2025, **29**, 101067.

7 K. Chauchan, R. Kaur and I. Chauhan, *Polym.-Plast. Technol. Mater.*, 2024, **63**, 913–938.

8 S. Nizamuddin, A. J. Baloch, C. Chen, M. Arif and N. M. Mubarak, *Int. Biodeterior. Biodegrad.*, 2024, **195**, 105887.

9 G. Chen, J. Li, Y. Sun, Z. Wang, G. A. Leeke, C. Moretti, Z. Cheng, Y. Wang, N. Li, L. Mu, J. Li, J. Tao, B. Yan and L. Hou, *Engineering*, 2024, **32**, 152–162.

10 C. Moretti, L. Hamelin, L. G. Jakobsen, M. H. Junginger, M. M. Steingrimsdottir, L. Høibye and L. Shen, *Resour. Conserv. Recycl.*, 2021, **169**, 105508.

11 G. Anderson and N. Shenkar, *Environ. Pollut.*, 2021, **268**, 115364.

12 B. Freeland, E. McCarthy, R. Balakrishnan, S. Fahy, A. Boland, K. D. Rochfort, M. Dabros, R. Marti, S. M. Kelleher and J. Gaughran, *Materials*, 2022, **15**, 2989.

13 T. Ramos-Hernández, J. R. Robledo-Ortíz, M. E. González-López, A. S. M. del Campo, R. González-Núñez, D. Rodrigue and A. A. Pérez Fonseca, *J. Appl. Polym. Sci.*, 2023, **140**, e53759.

14 L. Ranakoti, B. Gangil, S. K. Mishra, T. Singh, S. Sharma, R. A. Ilyas and S. El-Khatib, *Materials*, 2022, **15**, 4312.

15 M. S. Islam, Z. Lee, A. Shaleh and H. S. Soo, *Environ. Dev. Sustainability*, 2024, **26**, 10927–10944.

16 Sustainable packaging, https://www.consilium.europa.eu/en/press/press-releases/2024/12/16/sustainable-packaging-council-signs-off-on-new-rules-for-less-waste-and-more-re-use-in-the-eu/, accessed 7 January 2025.

17 F. Wang, Z. Nan, X. Sun, C. Liu, Y. Zhuang, J. Zan, C. Dai and Y. Liu, *Spectrochim. Acta, Part A*, 2022, **279**, 121376.

18 T. Leejarkpai, U. Suwanmanee, Y. Rudeekit and T. Mungcharoen, *Waste Manag.*, 2011, **31**, 1153–1161.

19 G. Kale, R. Auras, S. P. Singh and R. Narayan, *Polym. Test.*, 2007, **26**, 1049–1061.

20 T. D. Moshood, G. Nawanir, F. Mahmud, F. Mohamad, M. H. Ahmad and A. AbdulGhani, *Clean Eng. Technol.*, 2022, **6**, 100404.

21 S. Kwon, M. C. Zambrano, R. A. Venditti and J. J. Pawlak, *Int. Biodeterior. Biodegrad.*, 2023, **185**, 105671.

22 L. Ribba, M. Lopretti, G. M. de Oca-Vásquez, D. Batista, S. Goyanes and J. R. Vega-Baudrit, *Environ. Res. Lett.*, 2022, **17**, 033003.

23 A. M. Youssef and S. M. El-Sayed, *Carbohydr. Polym.*, 2018, **193**, 19–27.

24 J. D'Amario, W. Limsukon, A. Bher and R. Auras, *RSC Appl. Polym.*, 2025, **3**, 711–721.

25 W. Limsukon, M. Rubino, M. Rabnawaz, L.-T. Lim and R. Auras, *Polym. Degrad. Stab.*, 2023, **217**, 110537.

26 N. Hajilou, S. S. Mostafayi, A. L. Yarin and T. Shokuhfar, *AppliedChem*, 2024, **5**, 1.

27 A. Bher, Y. Cho and R. Auras, *Macromol. Rapid Commun.*, 2023, **44**, 2200769.

28 E. Castro-Aguirre, R. Auras, S. Selke, M. Rubino and T. Marsh, *Polymers*, 2018, **10**, 202.

29 P. Stloukal and P. Kucharczyk, *Polym. Degrad. Stab.*, 2017, **142**, 217–225.

30 D. Chauliac, P. C. Pullammanappallil, L. O. Ingram and K. T. Shanmugam, *J. Polym. Environ.*, 2020, **28**, 1503–1512.

31 H.-Y. Lin, S.-Y. Tsai, H.-T. Yu and C.-P. Lin, *J. Polym. Environ.*, 2018, **26**, 122–131.

32 J. Liu, C. Zhang, H. Huang, M. Yao, S. Li, J. Li, W. Zhang and J. Yin, *Int. J. Biol. Macromol.*, 2025, **291**, 139099.

33 E. Trofimchuk, V. Ostrikova, O. Ivanova, M. Moskvina, A. Plutalova, T. Grokhovskaya, A. Shchelushkina, A. Efimov, E. Chernikova, S. Zhang and V. Mironov, *Polymers*, 2023, **15**, 4017.

34 E. Castro-Aguirre, R. Auras, S. Selke, M. Rubino and T. Marsh, *Polym. Degrad. Stab.*, 2018, **154**, 46–54.

35 J. Oh, S. B. Park, C. Cha, D. K. Hwang, S.-A. Park, J. Park, D. X. Oh, H. Jeon and J. M. Koo, *Chemosphere*, 2024, **354**, 141729.

36 Y. Kara and K. Molnár, *J. Polym. Environ.*, 2023, **31**, 1398–1414.

37 M. L. Iglesias-Montes, M. Soccio, F. Luzi, D. Puglia, M. Gazzano, N. Lotti, L. B. Manfredi and V. P. Cyras, *Polymers*, 2021, **13**, 3171.

38 P. Brdlík, J. Novák, M. Borůvka, L. Běhálek and P. Lenfeld, *Polymers*, 2023, **15**, 140.

39 J. O'Loughlin, D. Doherty, B. Herward, C. McGleenan, M. Mahmud, P. Bhagabati, A. N. Boland, B. Freeland, K. D. Rochfort, S. M. Kelleher, S. Fahy and J. Gaughran, *Sustainability*, 2023, **15**, 15312.

40 N. F. Zaaba and M. Jaafar, *Polym. Eng. Sci.*, 2020, **60**, 2061–2075.

41 E. Castro-Aguirre, F. Iñiguez-Franco, H. Samsudin, X. Fang and R. Auras, *Adv. Drug Deliv. Rev.*, 2016, **107**, 333–366.

42 L. Liu, M. Xu, Y. Ye and B. Zhang, *Sci. Total Environ.*, 2022, **806**, 151312.

43 Z. Lin, T. Jin, T. Zou, L. Xu, B. Xi, D. Xu, J. He, L. Xiong, C. Tang, J. Peng, Y. Zhou and J. Fei, *Environ. Pollut.*, 2022, **304**, 119159.

44 H. Jiang, Y. Wang, J. Sun, Y. Mao, S. Que, Y. Lin, Y. Huang and X. Lei, *Environ. Geochem. Health*, 2024, **46**, 163.

45 Compostable packaging's relationship status with organics recyclers, https://www.wastedive.com/news/bpi-summit-compostable-packaging-usda-calrecycle/728240/, accessed 9 October 2025.

46 L. Gonzalez-Victoriano, E. Silva Camacho, J. D. Hernández-Varela, B. Arredondo-Tamayo, S. D. Gallegos-Cerda, J. J. Chanona-Pérez, F. Cervantes-Sodi and E. Martínez-Mercado, Sci. Total Environ., 2024, 955, 176763.

47 V. Goel, P. Luthra, G. S. Kapur and S. S. V. Ramakumar, J. Polym. Environ., 2021, 29, 3079–3104.

48 ISO 20200, https://www.iso.org/standard/81932.html, accessed 14 October 2025.

49 V. Gigante, G. Gallone, L. Aliotta and A. Lazzeri, Mater. Today Sustain., 2024, 28, 100953.

50 C. Maraveas, I. V. Kyrtopoulos and K. G. Arvanitis, Polymers, 2024, 16, 1104.

51 M. F. Cosate de Andrade, P. M. S. Souza, O. Cavalett and A. R. Morales, J. Polym. Environ., 2016, 24, 372–384.

52 M. R. Hasan, I. J. Davies, A. Pramanik, M. John and W. K. Biswas, Sustainable Manuf. Serv. Econ., 2024, 3, 100020.

53 I. Anderson, 3D Print. Addit. Manuf., 2017, 4, 110–115.

54 A. C. Pinho, A. M. Amaro and A. P. Piedade, Waste Manag., 2020, 118, 426–434.

55 A. Alexandre, F. A. Cruz Sanchez, H. Boudaoud, M. Camargo and J. M. Pearce, 3D Print. Addit. Manuf., 2020, 7, 237–247.

56 A. Pongwisuthiruchte and P. Potiyaraj, Mater. Today Sustainability, 2025, 31, 101134.

57 G. Embia, B. R. Moharana, A. Mohamed, K. Muduli and N. B. Muhammad, in New Horizons for Industry 4.0 in Modern Business, ed. A. Nayyar, M. Naved and R. Rameshwar, Springer International Publishing, Cham, 2023, pp. 253–272.

58 T. S. Woodson, Development, 2015, 58, 571–576.

59 A. Dey, I. N. Roan Eagle and N. Yodo, J. Mater. Process. Manuf. Sci., 2021, 5, 69.

60 M. A. Urbina, A. J. R. Watts and E. E. Reardon, Nature, 2015, 528, 479.

61 D. Doherty, K. D. Rochfort, M. Conaghan, J. O'Loughlin, B. Freeland, C. Cooling, D. Solola, Y. Brych, S. M. Kelleher, S. Fahy and J. Gaughran, Sustainable Mater. Technol., 2024, e00899.

62 J. O Loughlin, B. Herward, D. Doherty, P. Bhagabati, S. M. Kelleher, S. Fahy, B. Freeland, K. D. Rochfort and J. Gaughran, Heliyon, 2024, 10, e39846.

63 K. Ito, Japanese Pat., JPH05178977A, 1991.

64 ISO 17088, https://www.iso.org/standard/74994.html, accessed 14 October 2025.

65 L. Suárez, Z. Ortega, F. Romero, R. Paz and M. D. Marrero, J. Polym. Environ., 2022, 30, 4848–4862.

66 H. de la Rosa-Ramírez, M. Aldas, J. M. Ferri, F. Pawlak, J. López-Martínez and M. D. Samper, J. Polym. Environ., 2023, 31, 5462–5476.

67 L.-C. Leitner, T. Steiner, A. Greiner and R. Freitag, Microplastics, 2025, 4, 59.

68 S. Körber, K. Moser and J. Diemert, Polymers, 2022, 14, 384.

69 B. Cetiner, G. Sahin Dundar, Y. Yusufoglu and B. Saner Okan, Polymers, 2023, 15, 1085.

70 W. Ali, H. Ali, S. Gillani, P. Zinck and S. Souissi, Environ. Chem. Lett., 2023, 21, 1761–1786.

71 N. M. Ainali, D. Kalaronis, E. Evgenidou, G. Z. Kyzas, D. C. Bobori, M. Kaloyianni, X. Yang, D. N. Bikiaris and D. A. Lambropoulou, Sci. Total Environ., 2022, 832, 155014.

72 G. Gorrasi and R. Pantani, Polym. Degrad. Stab., 2013, 98, 1006–1014.

73 A. Magoń and M. Pyda, Polymer, 2009, 50, 3967–3973.

74 O. Vyavahare, D. Ng and S. L. Hsu, J. Phys. Chem. B, 2014, 118, 4185–4193.

75 N. A. Sukindar, A. S. H. Md Yasir, M. D. Azhar, M. A. Md Azhar, N. F. H. Abd Halim, M. H. Sulaiman, A. S. H. Ahmad Sabli and M. K. A. Mohd Ariffin, Heliyon, 2024, 10, e25508.

76 C. Arnold, D. Monsees, J. Hey and R. Schweyen, Materials, 2019, 12, 1970.

77 J. F. Macnamara Jr, A. Bher and R. Auras, ACS Omega, 2025, 10, 18936–18944.

78 N. K. Kalita, N. A. Damare, D. Hazarika, P. Bhagabati, A. Kalamdhad and V. Katiyar, Environ. Chall., 2021, 3, 100067.

79 J. Oh, S. B. Park, C. Cha, D. K. Hwang, S.-A. Park, J. Park, D. X. Oh, H. Jeon and J. M. Koo, Chemosphere, 2024, 354, 141729.

80 I. Grizzi, H. Garreau, S. Li and M. Vert, Biomaterials, 1995, 16, 305–311.

81 A. Melelli, D. Pantaloni, E. Balnois, O. Arnould, F. Jamme, C. Baley, J. Beaugrand, D. U. Shah and A. Bourmaud, Polymers, 2021, 13, 2225.

82 R. Pantani and A. Sorrentino, Polym. Degrad. Stab., 2013, 98, 1089–1096.

83 Y. Kobayashi, T. Ueda, A. Ishigami and H. Ito, Polymers, 2021, 13, 4324.

84 A. N. Mistry, B. Kachenchart, A. Wongthanaroj, A. Somwangthanaroj and E. Luepromchai, Polym. Degrad. Stab., 2022, 202, 110051.

85 D. Hidalgo-Carvajal, Á. H. Muñoz, J. J. Garrido-González, R. Carrasco-Gallego and V. Alcázar Montero, Polymers, 2023, 15, 3651.

86 V. Gil Muñoz, L. M. Muneta, R. Carrasco-Gallego, J. de Juanes Marquez and D. Hidalgo-Carvajal, Appl. Sci., 2020, 10, 8967.

87 G. Atakok, M. Kam and H. B. Koc, J. Mater. Res. Technol., 2022, 18, 1542–1554.

88 F. Carrasco, P. Pagès, J. Gámez-Pérez, O. O. Santana and M. L. Maspoch, Polym. Degrad. Stab., 2010, 95, 116–125.

89 M. Sedničková, S. Pekařová, P. Kucharczyk, J. Bočkaj, I. Janigová, A. Kleinová, D. Jochec-Mošková, L. Omaníková, D. Perďochová, M. Koutný, V. Sedlařík, P. Alexy and I. Chodák, Int. J. Biol. Macromol., 2018, 113, 434–442.

90 M. L. Iglesias-Montes, M. Soccio, F. Luzi, D. Puglia, M. Gazzano, N. Lotti, L. B. Manfredi and V. P. Cyras, Polymers, 2021, 13, 3171.

91 F. R. Beltrán, M. P. Arrieta, E. Moreno, G. Gaspar, L. M. Muneta, R. Carrasco-Gallego, S. Yáñez, D. Hidalgo-Carvajal, M. U. de la Orden and J. Martínez Urreaga, Polymers, 2021, 13, 1247.